THz-PULSE-TRAIN PHOTOINJECTOR

C.H. Chen[1], Y. C. Huang[1,2], K. Y. Huang[1], [1]Department of Electrical Engineering, National Tsinghua University, Hsinch 30013, Taiwan
W. K. Lau[2], A. P. Lee[2], [2]National Synchrotron Radiation Research Centre, Hsinchu 30076, Taiwan

Abstract

A THz-pulse-train photoinjector is under construction at the High-energy OPtics and Electronics (HOPE) Laboratory at National Tsinghua University, Taiwan. We show in this study that such a photoinjector is capable of generating periodically bunched MeV electrons with a bunching factor larger than 0.1 at THz frequencies for a total amount of 1 nC charges in a 10-ps time duration.

INTRODUCTION

In the past, many laboratories have demonstrated temporally compressed electron pulses by sending properly energy chirped electrons into a chicane magnet or alpha magnet [1]. Apart from the interest of generating a single short electron pulse, generation of a fast electron pulse train has recently attracted much attention for generating high-brightness electron radiation. For example, Neumann *et al.* generated 2-4 electron bunches with a sub-THz pulse rate by using a modulated laser beam to illuminate the photocathode of an electron gun [2]. Power *et al.* proposed the use of birefringence crystals to split the driver laser pulse of a photoinjector to induce the emission of a fast electron pulse train from a photocathode [3]. To generate a long pulse train and ease the pulse-rate tuning, here we propose a laser-beat-wave photoinjector.

Figure 1 illustrates the proposed THz-pulse-train (TPT) photoinjector. The TPT photoinjector consists of three major elements, a photocathode accelerator, an emittance compensating coil, and a beat-wave driver laser. The beat-wave laser generates a laser radiation containing the beating of two frequency components separated by THz frequencies. The two laser components are derived from mixing of two amplified diode lasers, one with a fixed frequency and one with a tunable frequency. The beat frequency of the laser and thus the electron pulse rate can be tuned by varying the frequency of the tunable diode laser relative to that of the fixed-frequency one. By using such a tuning scheme, the proposed TPT photoinjector has a pulse rate tuning range exceeding 10 THz [4]. The TPT photoinjector uses the laser beat pulses to induce the emission of a fast electron pulse train, which does not add any energy spread like other schemes using magnetic components. In the following, we will present our simulation and theoretical study of the TPT photoinjector by taking a 1.6-cell S-band electron gun [5] as an example. The bunching factor is the key parameter describing how well an electron beam is bunched. We calculate in the following the bunching spectrum for the electrons from the TPT photoinjector subject to a typical setup of a photoinjector.

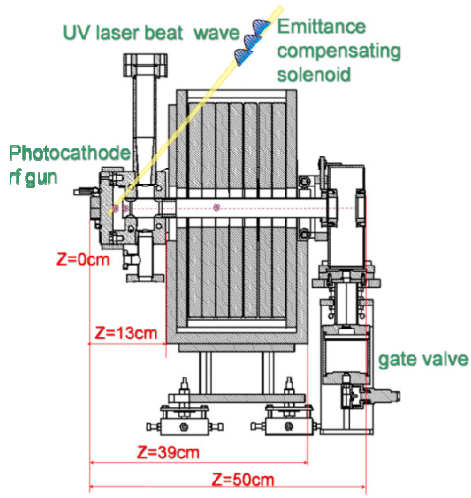

Figure 1: The proposed TPT photoinjector comprises a UV beat-wave laser, 1.6-cell S-band photocathode electron gun, and an emittance compensation coil. The beat pulses of the laser induce the emission of fast electron pulses from the photocathode of the electron gun.

BEAT-WAVE LASER

Figure 2 shows the design concept of the beat-wave laser driving the electron gun. The laser beat wave is combined from two diode lasers near 1.56 um with their frequencies differing by THz. One diode laser has a fixed frequency and the other is fully tunable between 1.5 and 1.6 μm, corresponding to a tuning range of 12 THz. An optical parametric amplifier (OPA) pumped by a mode-locked Nd:YVO_4 laser boosts up the energy of the beat-wave seed to a kW-power level in a 10 ps pulse width. We then double the frequency of the amplified beat pulse near 1.5 μm to 780 nm in a second harmonic generator (SHG). The 780-nm beat-wave laser can be readily amplified in a Ti:sapphire laser amplifier. A third harmonic generator (THG) following the Ti-sapphire laser amplifier converts the amplified beat wave at 780 nm to UV to drive the photocathode electron gun.

If the laser amplifier is linear, then the intensity of the beat-wave laser at the output contains only two frequency components beating at a frequency ω_b in a Gaussian envelope. The intensity of such a two-frequency (2-f) beat wave can be described by the expression:

$$I(t) = I_0 e^{-t^2/(2\sigma_M^2)} \cos^2(\omega_c t + \phi_1) \cos^2(\omega_b t/2 + \phi_2), \qquad (1)$$

where I_0 is the peak intensity, t is the time variable, σ_M is the rms width of the Gaussian pulse or the macro-pulse, ω_c is the center frequency of the two beat-wave components, and $\phi_{1,2}$ are arbitrary phases. For a Gaussian pulse with a nominal 10 ps full-width at half-maximum

(FWHM), the rms pulse width of the Gaussian pulse is σ_M = 4.25 ps. The center laser frequency ω_c or the laser photon energy $\hbar\omega_c$ must be large enough to overcome the work function of the cathode material, where $\hbar = h/2\pi$, with h being the Planck's constant. The photoemission at the cathode follows the low-frequency intensity envelope

$$I_e(t) = \frac{I_0}{2} e^{-t^2/(2\sigma_M^2)} \cos^2(\omega_b t/2 + \phi_2) \quad (2)$$

where $1/\omega_b$ is significantly longer than the characteristic time of photoemission. The carrier envelope phase ϕ_2 is not important for a large number of electron pulses excited by the beat pulses. We therefore drop ϕ_2 from Eq. (2) for our following studies.

The electron bunching factor is a figure of merit to describe how well an electron beam is bunched at a particular frequency. The bunching spectrum is defined as

$$B_f(\omega) = \left| \sum_{m=1}^{N} e^{j\omega t_m} \right| / N, \quad (3)$$

where N is the total number of particles, $j = \sqrt{-1}$ is the imaginary unit, and t_i is the temporal location of the ith electrons. For a continuous distribution function of the electrons $f(t)$, Eq. (3) becomes a Fourier transform of $f(t)$, provided that the normalization $\int_{-\infty}^{\infty} f(f)dt = 1$ is applied. Since the photoemission probability follows the low-frequency intensity envelope of the incident laser, the bunching factor at the cathode of the photoinjector is given by

$$B_f(\omega) = \left| \int_{-\infty}^{\infty} I_e(t) e^{i\omega t} dt \right| / \int_{-\infty}^{\infty} I_e(t) dt, \quad (4)$$

For the intensity envelope of the two-frequency beat wave given in Eq. (2), the bunching factor at the cathode, according to Eq. (4), is:

$$B_f(\omega) = \frac{[e^{-\frac{1}{2}\sigma_M^2\omega^2} + \frac{1}{2}e^{-\frac{1}{2}\sigma_M^2(\omega-\omega_b)^2} + \frac{1}{2}e^{-\frac{1}{2}\sigma_M^2(\omega+\omega_b)^2}]}{(1+e^{\frac{-1}{2}\omega_b^2\sigma_M^2})}, \quad (5)$$

In the limit of many bunches in a macro-pulse or $\sigma_M >> 1/\omega_b$, the maximum bunching factor at the bunch frequency $\omega = \omega_b$ is 0.5 for a 2-f beat-wave driver laser.

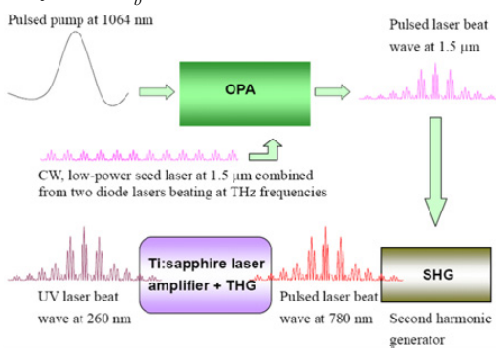

Figure 2: The proposed beat-wave laser system for driving the photoinjector.

LABEW PHOTOINJECTOR

The particle acceleration process in a photoinjector could modify the initial particle distribution at the cathode and thus modify the bunching spectrum at the output of the accelerator. In this subsection, we present the simulated performance of the 2-f TPT photoinjector with a 100MV/m peak acceleration gradient by using the simulation code ASTRA [6]. The selected beat frequency for the driver laser is $\omega_b/2\pi$ = 2 THz. The initial electron pulses at the cathode follow the laser-intensity profile described by Eq. (2).

Fig. 3 shows (a) the solenoid field profile with a peak field of 2.66 kG at z = 27 cm, (b) the rms beam radius, (c) the normalized beam emittance, and (d) the energy spread versus distance for the pulse-train acceleration and propagation between the photocathode and the solenoid exit. The average output energy of the electrons is 4.6 MeV (γ = 10). It can be seen that, despite the use of the compensating coil, the emittance grows from 5 to 8.2 π mm mrad due to the large space-charge force in the low-energy beam. The solenoid field was not fully optimized to reduce the emittance, but was used to provide a beam focus at z = 50 cm (the entrance of an undulator). The energy spread also increases slightly over z, again, due to the space-charge force

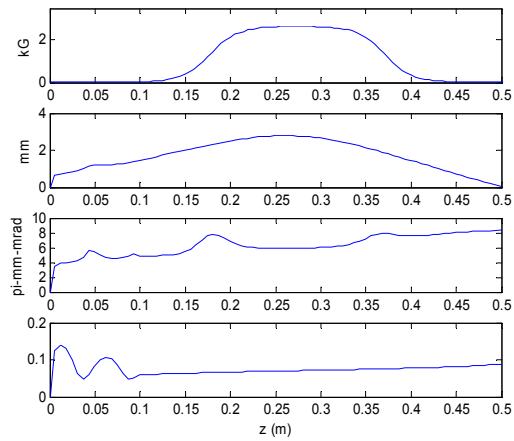

Figure 3: (a) Solenoid field, (b) rms beam radius, (c) normalized emittance, and (d) energy spread versus axial distance z for 2-THz electron pulses accelerated by a peak field gradient of 100 MV/m in the photoinjector.

The electron bunching can be quantitatively described by the bunching spectrum defined by Eq. (4). Fig. 4 shows the bunching spectra of the particles calculated at the cathode (z = 0), at the gun exit (z=12 cm), and at the solenoid exit (z=50 cm) for 1 nC charges, and at the solenoid exit for 0.1 nC charges. The initial bunching factor of 0.5 at 2 THz agrees well with the theory in Eq. (5). It can be seen from Fig 4 that the particle acceleration process indeed lowers the bunching factor, and broadens the bunching spectrum for such a 2-f LABEW photoinjector. The blue shift of the output bunching spectrum is due to velocity bunching during acceleration. The longitudinal pulse compression and thus the blue

shift of the bunching spectrum are more evident for the 0.1 nC beam, in which the longitudinal space-charge force is smaller. For the 1 nC beam, it is interesting to note that the drift space between z = 12 cm and 50 cm helps to translate some energy modulation into a slightly higher bunching amplitude at 2.3 THz. Despite some debunching during acceleration and propagation, the bunching factor at the fundamental bunch frequency is still kept above 10% for 1 nC acceleration charges. The bunching factor of the 0.1 nC output beam is twice as large as that of the 1-nC output beam.

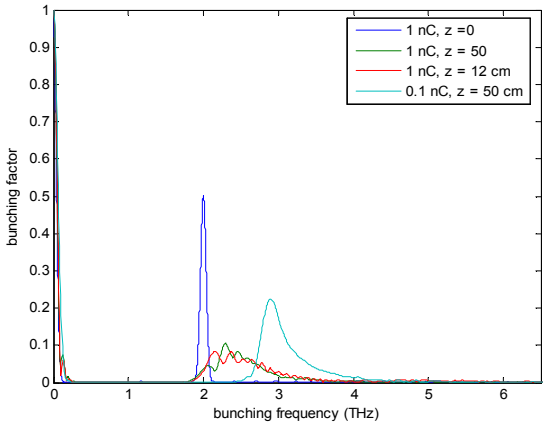

Figure: 4. Bunching spectra for particles at z = 0, 12 cm, and 50 cm with 1-nC charges in the beam, and for particles at z = 50 cm with 0.1 nC in the beam. The blue shift of the bunching spectrum is due to velocity bunching during acceleration. The micro-pulses are better retained in a low-charge beam.

CONCLUSION

An electron pulse train with THz pulse rates finds applications in areas such as generating electron superradiance, and loading or driving a plasma-wave accelerator. As presented in this paper, we have studied a laser-beat-wave photoinjector that is capable of producing an electron pulse train with a broadly tunable pulse rate in the THz range. The idea was to use a tunable beat-wave laser incident on the cathode of a photoinjector to induce photoemission of THz electron pulses. Magnetically compressing an energy-chirped pulse train from such a TPT photoinjector could further extend the electron pulse rate to hundreds of THz.

We have also identified a highly effective and efficient beat-wave laser system suitable for driving such a photoinjector. The laser beat pulses are generated by amplifying two low-power diode lasers beating at THz frequencies. Tuning the beat-pulse rate is achieved by varying the relative frequency between the two diode lasers. We used the ASTRA code to model the performance of an S-band TPT photoinjector. In general, we found that a bunching factor larger than 0.1 is achievable at THz frequencies for 1 nC acceleration charges. The space-charge force plays a crucial role in degrading the micro-bunches during acceleration. With 10-times reduced acceleration charges, the bunching factor at the bunch frequency increases more than twice. Velocity bunching in a photoinjector can also shift the bunch frequency during particle acceleration. However, this frequency shift can be easily compensated for by varying the beat frequency of our tunable driver laser. Use of the pulse train from a TPT photoinjector to generate electron superradiance is presented in another paper (TUPE044).

ACKNOWLEDGMENTS

This work is jointly supported by the National Science Council, under Contract NSC 97-2112-M-007-018-MY2; the National Synchrotron Radiation Research Center, under Project 955LRF01N; and National Tsinghua University, under Project 98N2534E1.

REFERENCES

[1] J.B. Rosenzweig, N. Barov, E. Colby, IEEE Trans. Plasma Sci. 24 (1996) 409.
[2] J.G. Neumann, P.G. O'Shea, D. Demske, W.S. Graves, B. Sheehy, H. Loos, G.L. Carr, Nucl. Instr. and Meth. Phys. Res. A 507 (2003) 498.
[3] J.G. Power, C. Jing, Temporal laser pulse shaping for RF photoinjectors: the cheap and easy way using UV birefringent crystals, in: Proceedings of the Advanced Accelerator Concept Workshop, Santa Cruz, CA, USA, July 27–Aug. 3, 2008.
[4] Y.C. Huang, Int. J. Mod. Phys. B 21 (2007) 287.
[5] D.T. Palmer, X.J. Wang, I. Ben-Zvi, R.H. Miller, Proc. IEEE Part. Accel. Conf. 3 (1997) 2846.
[6] K.Floettmann, ASTRA User Manual, available at: http://www.desy.de/ mpyflo/Astra_documentations